

Chick Dach1 interacts with the Smad complex and Sin3a to control AER formation and limb development along the proximodistal axis

Yasuyuki Kida^{1,2}, Yukiko Maeda¹, Tomoki Shiraishi¹, Takayuki Suzuki^{1,2} and Toshihiko Ogura^{2,*}

¹Graduate School of Biological Sciences, Nara Institute of Science and Technology, 8916-5, Takayama, Ikoma, Nara, 630-0101, Japan

²Department of Developmental Neurobiology, Institute of Development, Aging and Cancer, Graduate School of Medicine, Tohoku University, 4-1, Seiryō, Aoba, Sendai, 980-8575, Japan

*Author for correspondence (e-mail: ogura@idac.tohoku.ac.jp)

Accepted 5 May 2004

Development 131, 4179-4187
Published by The Company of Biologists 2004
doi:10.1242/dev.01252

Summary

Based on recent data, a new view is emerging that vertebrate Dachshund (Dach) proteins are components of Six1/6 transcription factor-dependent signaling cascades. Although *Drosophila* data strongly suggest a tight link between Dpp signaling and the *Dachshund* gene, a functional relationship between vertebrate Dach and BMP signaling remains undemonstrated. We report that chick Dach1 interacts with the Smad complex and the co-repressor mouse Sin3a, thereby acting as a repressor of BMP-mediated transcriptional control. In the limb, this antagonistic action regulates the formation of the apical ectodermal ridge (AER) in both the mesenchyme and the

AER itself, and also controls pattern formation along the proximodistal axis of the limb. Our data introduce a new paradigm of BMP antagonism during limb development mediated by Dach1, which is now proven to function in different signaling cascades with distinct interacting partners.

Supplementary data available online

Key words: Dachshund, Smad1, Sin3a, Limb development, AER, Chick

Introduction

Pattern formation of the limb bud is controlled along three-dimensional axes. Establishment of the dorsoventral (DV) and the anteroposterior (AP) axes is regulated by organizing centers set up in the limb bud (Johnson and Tabin, 1997; Martin, 1998; Schwabe et al., 1998). Engrailed 1 (*En1*) and *Wnt7a* are expressed in the ventral and dorsal ectoderm, respectively. *En1* represses expression of *Wnt7a*. *Lmx1b*, a LIM-homeodomain transcription factor, is induced in the dorsal mesenchyme by *Wnt7a* (Cygan et al., 1997). The actions of these factors establish the boundary between the dorsal and ventral ectoderm. Consequently, the expression of *Notch1* and *Fgf8* occurs on this boundary, making a distinct structure, the apical ectodermal ridge (AER) (Hayashi et al., 1996; Capdevila and Izpisua Belmonte, 2001).

Pattern formation along the AP axis is controlled by the zone of polarizing activity (ZPA), located in the posterior margin of the limb bud. Sonic hedgehog (*Shh*) is expressed in the ZPA and exerts its polarizing activity. Expression of *Shh* is maintained by *Fgf4* in the AER; hence, tight communication between the ZPA and the AER is important for pattern formation. Limb outgrowth is maintained by FGF8 in the AER, thereby controlling morphogenesis along the PD axis (Rubin and Saunders, 1972). Thus, the Shh/FGF regulatory loop ensures coordinated growth and patterning along the AP and PD axes.

Several BMP genes are also expressed in the AER and underlying mesenchyme, playing pivotal roles in the control

of proliferation, differentiation and programmed cell death (Yokouchi et al., 1996). When Noggin, a BMP antagonist, was misexpressed, anterior extension of the AER and loss of its asymmetry was observed (Pizette and Niswander, 1999), establishing a BMP antagonist as an apical ectodermal maintenance factor (AEMF) (Zwilling, 1956). When a constitutively active BMP receptor was misexpressed, the AER and its *Fgf8* expression were lost, resulting in severe truncation (Pizette et al., 2001; Ahn et al., 2001). Both gain- and loss-of-function approaches revealed that BMP signaling regulates pattern formation along the DV and PD axes. However, the expression pattern of *Noggin* indicates that this factor is not the bona fide AEMF. Another BMP antagonist, Gremlin, is expressed in the limb bud, suggesting its involvement in the AEMF pathway. As expected, misexpression of Gremlin antagonized BMP signaling and induced hyperplasia of the AER (Capdevila et al., 1999; Merino et al., 1999; Zuniga et al., 1999). In addition, Gremlin makes a tight regulatory loop between the Shh and FGF signaling cascades, rendering this factor an excellent AEMF candidate.

Dachshund (*Dac*) was identified as one of the retinal determinants in *Drosophila*. Null mutation of *Dac* results in reduction or complete loss of compound eyes. *Dac* mutants have short legs, with condensation of the femur, tibia and proximal tarsi, compatible with the expression pattern of *Dac* in the intermediate domain of the leg disc. In addition, cell

death is increased (Mardon et al., 1994). *Dac* expression overlaps with that of *dpp* in both the morphogenetic furrow (MF) and leg discs, making a tight regulatory loop. This suggests that *dpp* and *Dac* are functionally related to achieve the correct formation of legs and eyes (Gonzalez-Crespo et al., 1998). Furthermore, *eyeless* (*eye*), *eyes absent* (*eya*), *sine oculis* (*so*) and *dac* are components of the pathway of compound eye formation (Desplan, 1997; Wawersik and Maas, 2000), making a complex network (Chen et al., 1997; Pignoni et al., 1997). Recently, vertebrate homologues of *eye*, *eya*, *so* and *dac* have been identified: *Pax6*, *Eya1-Eya4*, *Six1-Six9*, and *Dach1* and *Dach2*, respectively (Quiring et al., 1994; Oliver et al., 1995; Hammond et al., 1998; Mishima and Tomarev, 1998; Borsani et al., 1999; Heanue et al., 1999; Kozmik et al., 1999; Lopez-Rios et al., 1999). (Expression patterns of chick *Dach1* can be found at <http://dev.biologists.org/supplemental>.)

We describe a novel antagonistic function of chick *Dach1* on BMP signaling. We show that the nuclear events involving *Dach1* and BMP signaling control pattern formation along the PD axis and maintenance of the AER.

Materials and methods

Cloning of the chick *Dach1* gene and in situ hybridization

The chick *Dach1* gene was isolated by screening a chick eye cDNA library with a probe derived from the mouse *Dach1* plasmid. The mouse *Dach1* gene was amplified by RT-PCR based on the published databases. Whole-mount and section in situ hybridization was performed as described (Wilkinson and Nieto, 1993; Koshiba-Takeuchi et al., 2000).

Cell culture, transfections and luciferase assay

C2C12 and Cos7 cells were maintained in high-glucose DMEM supplemented with 10% FCS. Transient transfection was performed using lipofectamine (Invitrogen) or polyethylenimine (Polysciences). In all transfection experiments, the total amount of transfected DNA was kept constant by adding an appropriate amount of empty vector. C2C12 cells (1×10^4 cells/well in 24-well tissue culture plates) were transfected with various combinations of plasmids: 200 ng of reporter constructs (*Xvent-2-Luc* or *4R-UAS-Luc* plasmid), 200 ng of β -galactosidase expression plasmids, 25-500 ng of various expression constructs containing *Dach1*, Gal4-DBD fused *Dach1*, BMP4, Smad1, Gal4-DBD-fused Smad1 (a kind gift from Dr Miyazono), mouse Sin3a, HDAC1 and N-CoR (a kind gift from Dr Ishii). Forty hours after transfection, cells were lysed, and lysates were subjected to luciferase assay. Luciferase activities were measured by Luminescencer-JNR (ATTO). β -Galactosidase activities were measured to standardize the transfection efficiency.

Immunoprecipitation and western blotting

Cos7 cells were transfected with expression plasmids containing hemagglutinin (HA)-tagged *Dach1* or the DD2 domain of *Dach1* along with Flag-tagged Smad1 or Flag-tagged mouse Sin3a. Transfected cells were harvested 40 hours after transfection, then lysed in lysis buffer [50 mM HEPES (pH 7.5), 250 mM NaCl, 0.2 mM EDTA, 10 μ M NaF, 0.5% NP-40]. Lysates were immunoprecipitated using an anti-HA antibody (Covance). Immunoprecipitants were subjected to SDS-PAGE, and western blot analysis was performed using an anti-Flag antibody (Sigma) and ECL detection reagents (Amersham).

In ovo electroporation and bead implantation

For electroporation, a BTX T-820 electroporator (BTX, San Diego)

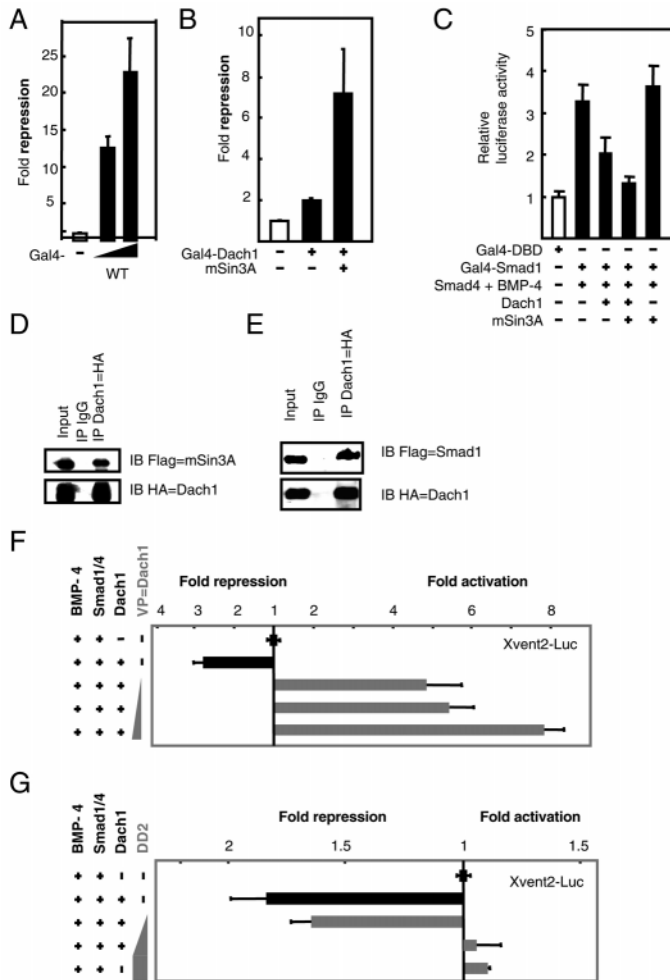
and pulse monitor (Meiwa Shoji, Japan) were used. Fertilized eggs were purchased from Takeuchi and Yamagishi poultry farms (Nara, Japan). Platinum electrodes (Muramatsu, Japan) and a sharpened tungsten needle (Nilaco) were used as an anode and a cathode, respectively. An anode was inserted beneath the endoderm, and a cathode was placed on the surface of the embryos. For ectodermal expression, DNA solution was poured over the ectoderm with a sharp glass pipette, and electric pulses were applied. Mesodermal expression was described previously (Takeuchi et al., 2003). Heparin-acrylic beads (diameter 100-160 μ m; Sigma) soaked for 1 hour at room temperature in recombinant BMP4 (0.5 mg/ml) were implanted into the limb buds.

Results

First, we constructed a *Gal4-DNA binding domain (DBD)-Dach1* fusion gene, and transfected it into Cos-7 cells along with the *4R-UAS-Luc* reporter plasmid. Robust repression of luciferase activities was observed in a dose-dependent manner (WT in Fig. 1A), suggesting that *Dach1* acts as a repressor, compatible with previous studies (Li et al., 2002; Wu et al., 2004). Next, we examined its putative interaction with mouse Sin3a, one of the components of a co-repressor complex (Fig. 1B). When a low amount of Gal4-*Dach1* was expressed in Cos-7 cells, weak repression of luciferase activity was observed. However, addition of a mouse Sin3a expression plasmid strongly enhanced this repressor activity, suggesting that *Dach1* interacts with Sin3a. To confirm further, we performed a similar luciferase assay using the *4R-UAS-Luc* reporter (Fig. 1C). Co-expression of Gal4-Smad1, Smad4 and BMP4 activated this reporter, and addition of *Dach1* repressed it (Fig. 1C). As expected, co-expression of mouse Sin3a further repressed the BMP4-mediated activation of *4R-UAS-Luc*, whereas this repression was cancelled when *Dach1* was removed, suggesting that Sin3a is involved in the *Dach1*-mediated repression.

Next, we again examined the interaction between mouse Sin3a and *Dach1*, using an immunoprecipitation assay. *Dach1* and mouse Sin3a were tagged with HA and Flag, respectively, then expressed in Cos-7 cells. An irrelevant IgG antibody did not precipitate either mouse Sin3a or *Dach1* (IP IgG, Fig. 1D). By contrast, when HA-tagged *Dach1* was immunoprecipitated, Flag-tagged mouse Sin3a was detected in the precipitants (IB Flag=m Sin3a in Fig. 1D). To examine whether *Dach1* interacts with Smad1, we performed the same co-immunoprecipitation assay. With an irrelevant antibody (IP IgG in Fig. 1E), neither Smad1 nor *Dach1* was detected. By contrast, when immunoprecipitation was performed with the anti-HA antibody to precipitate *Dach1*, both Smad1 and *Dach1* were detected (IP *Dach1*=HA/Flag=Smad1 and HA=*Dach1*, respectively, Fig. 1E), indicating that *Dach1* and Smad1 make a complex in Cos-7 cells. As *Dach1* binds to Smad4 (Wu et al., 2004), Smad4 might be involved in the formation of a ternary complex of *Dach1*, Smad1 and Smad4. Compatible with this, when purified proteins were used in a similar co-immunoprecipitation assay, an interaction between *Dach1* and Smad4 was stronger than that between *Dach1* and Smad1 (data not shown).

We further investigated whether *Dach1* modulates BMP signaling. We transfected an *Xvent2* promoter-luciferase reporter plasmid (*Xvent2-Luc*) (Hata et al., 2000) into C2C12 cells, together with expression plasmids of *BMP4*, *Smad1* and



Smad4. When a full-length Dach1 was co-expressed, luciferase activities were repressed (Fig. 1F). We constructed a transcriptionally active Dach1 by fusing the VP16 transactivation domain at the N-terminal end of Dach1 (VP=Dach1). As Dach1 makes a repressor complex, VP=Dach1 should form a transcriptional active complex. When VP=Dach1 was co-expressed, the *Xvent2* promoter was activated strongly, even in the presence of Dach1 (Fig. 1F). This suggests that VP=Dach1 acts as a transcriptionally active form and abrogates the Dach1-mediated transcriptional repression.

Comparison of *Drosophila* *Dac* and vertebrate Dach1 identified two highly conserved domains in the amino and C termini (DD1/DS and DD2/EYA domains, respectively) (Li et al., 2002; Wu et al., 2004). Our data indicate that mouse Sin3a binds directly to DD2 (data not shown), as previously reported (Li et al., 2002). As HDAC and NCoR bind to DD1 (Li et al., 2002), a synergistic interaction between DD1 and DD2 might be necessary for the formation of the functional co-repressor complex. In addition, DD2 binds to Smad1 (data not shown) and Smad4 (Wu et al., 2004). Based upon these observations, we speculated that DD2 per se blocks the synergistic action between Smad1 and Dach1. To confirm this hypothesis, we assessed the function of the DD2 construct in the *Xvent2*-luciferase context (Fig. 1G). When the full-length Dach1 was co-expressed with BMP4, Smad1 and Smad4, repression of

Fig. 1. (A) Cos-7 cells were transfected with increasing amounts of an expression vector containing the Gal4 DNA-binding domain (DBD) fused to full-length Dach1 (Gal4-WT), along with the 4R-UAS-Luc reporter plasmid, which contains four Gal4-DBD-binding motifs. Transcription was repressed by Gal4-WT in a dose-dependent manner (12.5- to 23-fold repression). (B) Using the same reporter, a low amount of Gal4-Dach1 was expressed in Cos-7 cells, resulting in weak repression. However, co-expression of mouse Sin3a strongly enhanced the repressor activity. (C) Co-expression of Gal4 DBD-Smad1 and BMP4 activated the 4R-UAS-Luc reporter. Expression of Dach1 weakened this BMP4-mediated activation. Addition of mouse Sin3a further repressed this activation. When Dach1 expression was removed, mouse Sin3a-mediated repression was no longer observed. (D) An immunoprecipitation assay was carried out using HA-tagged Dach1 and Flag-tagged mouse Sin3a expressed in Cos-7 cells. An irrelevant IgG did not precipitate either Dach1 or Sin3a (IP IgG). When the anti-HA antibody was used, both Dach1 and Sin3a were detected (IP Dach1=HA) by the anti-Flag antibody (IB Flag=mSin3a) and the anti-HA antibody (IB HA), respectively. Input, 5% of the extract used in this immunoprecipitation assay. (E) Flag-tagged Smad1 and HA-tagged Dach1 were co-expressed in Cos-7 cells, and cell lysates were immunoprecipitated with the anti-HA antibody or an irrelevant IgG (as a negative control). In the precipitant of the irrelevant IgG, neither Smad1 nor Dach1 was detected (IP IgG). By contrast, both Smad1 and Dach1 were present in the precipitant when the anti-HA antibody was used for IP (IP Dach1=HA). Input, 5% of the extract used in this immunoprecipitation assay. (F) Addition of Dach1 repressed the BMP-4/Smad1/Smad4-mediated transcription of the *Xvent2*-Luc reporter. Co-expression of VP=Dach1 activated this reporter even in the presence of Dach1. (G) By contrast, co-expression of DD2 did not activate this promoter, but instead cancelled the Dach1-mediated repression.

this promoter became evident. Interestingly, co-transfection of increasing amounts of the DD2 expression construct abrogated this Dach1-mediated repression. This suggests that DD2 per se acts as a dominant-negative in the BMP/Smad1/Sin3a-mediated transcriptional control. Nonetheless, in contrast to VP=Dach1 (Fig. 1F), DD2 did not activate the *Xvent2* promoter, but instead de-repressed the Dach1-mediated repression. From these observations, we speculate that using these two different constructs, we can investigate the functional roles of Dach1 with two different approaches. Namely, VP=Dach1 activates the BMP/Smad1-mediated transcription in a manner opposite to the normal Dach1, and DD2 de-represses its action, acting as a dominant-negative form.

As reported previously, the extracellular molecule Gremlin acts as a BMP antagonist (Capdevila et al., 1999). To confirm whether this extracellular antagonism sets up a 'BMP-zero status' in the limb buds, we stained sections of embryos with an anti-phosphorylated Smad1/5/8 antibody and found weak but distinct signals in the ectoderm and mesoderm of the limb (data not shown). These observations suggest that BMP signaling is weak but active in both the ectoderm and the mesoderm of the limb buds, despite the expression of Gremlin. This also suggests that Dach1 exerts its action with the BMP signal, which is attenuated by Gremlin. Hence, we could alter the BMP/Smad1/Dach1-mediated transcriptional control by the transcriptionally active VP=Dach1 and the dominant-negative DD2.

VP=Dach1 in the limb buds

Next, we misexpressed VP=Dach1 in the surface ectoderm at stages 8–11 (top insets in Fig. 2). At stage 19, expression of *Fgf8* was faint and blurred (Fig. 2A,B). At stage 24, severe deformities were seen in the distal ectoderm where strong enhanced green fluorescent protein (EGFP) signals derived from co-electroporated pCAGGS-EGFP were observed (Fig. 2C,D). Compatible with this, expression of *Fgf-8* was distorted and lost in the central part (Fig. 2E). A gap was also found in expression of *Bmp7* in the AER (Fig. 2F), and mesenchymal *Fgf10* expression was repressed (Fig. 2G). By contrast, *Shh* expression in the posterior part was not affected, although severe deformity was evident in the distal end (Fig. 2H).

At later stages, severe truncation of distal structures was obtained. In the leg, the distal autopod structure was completely lost, leaving the stylopod and zeugopod normal (Fig. 2I,J). These phenotypic changes resemble those observed when BMP-soaked beads were implanted or a constitutively active BMP receptor was misexpressed (Macias et al., 1997; Zou et al., 1997). These results indicate that VP=Dach1 affects the formation of the AER, resulting in the loss of the distal structures.

DD2 in the limb buds

Next, we misexpressed DD2 in the limb mesenchyme at stages 13–15 (top insets in Fig. 3). Electroporation was monitored by the EGFP signals derived from the co-injected pCAGGS-EGFP (Fig. 3A). At stage 19, 24 hours after electroporation, repression of *Fgf10* first became evident in the anterior side

(Fig. 3B). At this stage, repression of *Wnt5a* was also observed in the anterior domain with deformation of the AER (Fig. 3C).

As BMP signaling is required for the formation of the AER and the dorsoventral patterning of the limb (Barrow et al., 2003; Pizette et al., 2001), we examined the expression of marker genes after DD2 misexpression. At stage 19, *Fgf8* expression became blurred, without making sharp boundaries on its dorsal and ventral sides (Fig. 3D). Similar changes were observed in *En1* and *Msx2* expression (Fig. 3E,F). At stage 24, broadening of the irregular *Fgf8*-positive domain was found, with an *Fgf8*-negative line inside of the AER (Fig. 3G). By contrast, *Wnt7a* and *Lmx1b* were expressed dorsally (Fig. 3H,I), and *Bmp7* and *Msx2* were expressed ventrally (Fig. 3J,K). However, thickening of the ectoderm was evident near the margin of the expression of these markers (red arrowheads, Fig. 3H-K), making the AER structure unclear.

In severe cases, invagination of the thick epithelium was observed at stage 20 (red arrowhead in Fig. 4A). In such limbs, *Fgf8* expression was detected in this invaginated part (Fig. 4B), suggesting that the AER was formed, but invaginated in the underlying mesenchyme. Cyclin D1 was expressed normally in the mesenchyme, suggesting that this invagination was not caused by mesenchymal growth arrest.

Next, we detected β III-tubulin proteins in the limb buds. When stained with an anti-TuJ1 antibody, signals were observed in the motoneurons entering the proximal part of the limb and the ventral limb epithelium (Fig. 4D). In the dorsal epithelium, TuJ1 staining was faint or not observed. In the DD2-misexpressed limb, TuJ1 staining was evident in the ventral and the invaginated epithelia (Fig. 4E). When this image was magnified, clear invagination

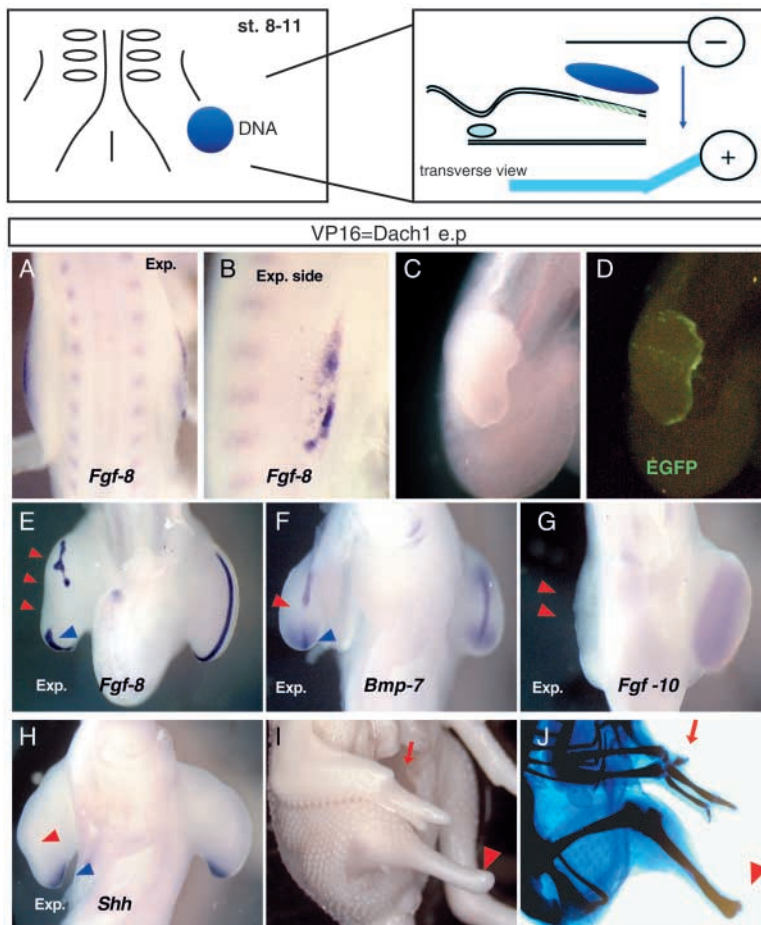


Fig. 2. VP=Dach1 was misexpressed in the ectoderm by pouring the plasmid solution over the ectoderm. Diagrams

at the top show the experimental design of electroporation. (A) A dorsal view of an electroporated limb bud on the right-hand side (Exp.) compared with a normal limb bud on the left. Expression of *Fgf8* is obscure. (B) In a lateral view, *Fgf8* expression is faint and blurred without making a clear boundary. (C) At stage 24, a severe depression was evident in the dorsal end of the limb bud. (D) Strong EGFP signals, which were derived from co-electroporated pCAGGS-EGFP, were observed in the ectoderm. (E) In such limb buds, *Fgf8* expression was lost in the central part and deformed in the anterior (red arrowheads), whereas *Fgf8* was normally expressed in the posterior (blue arrowhead). (F) Expression of *Bmp7* was also lost in the central part (red arrowhead) and in the anterior mesenchyme, but was normal in the posterior area (blue arrowhead). (G) Mesenchymal expression of *Fgf10* was repressed with inhibition of the limb outgrowth (red arrowheads). (H) *Shh* was expressed normally posteriorly (blue arrowhead). A depression similar to C was evident in the distal end (red arrowhead). (I) At stage 37, distal truncation was obtained. In the wing, where misexpression of VP=Dach1 was weak, truncation of digit II was evident. In the leg, where misexpression was extensive, distal autopod structures were completely missing (red arrowhead). (J) Alcian Blue staining of these limbs revealed a short digit II in the wing (red arrow) and the complete loss of digits in the leg (red arrowhead). Approximately 60% of the misexpressed limbs showed these phenotypes ($n=242$).

was observed, which was surrounded by the EGFP signals derived from the co-expressed pCAGGS-EGFP (Fig. 4F,G). This suggests that the mesenchymal misexpression of DD2 induced elongation and extensive folding of the ventral epithelium. Expression of *Fgf8* was not observed in this elongated epithelium, but was detected in a more distal part (Fig. 4H). In this case, formation of the AER was abnormal and depressed in the mesenchyme. When analyzed in whole mount, the *Fgf8*-positive region was broad and flat (Fig. 4I). The invagination of the ventral epithelium split the limb buds, resulting in two protrusions, as shown in Fig. 4J,K. Expression of *Shh* and *Gremlin* was detected in both protrusions, although expression of *Shh* and *Gremlin* was weak in the ventral and the dorsal sides, respectively (Fig. 4J,K).

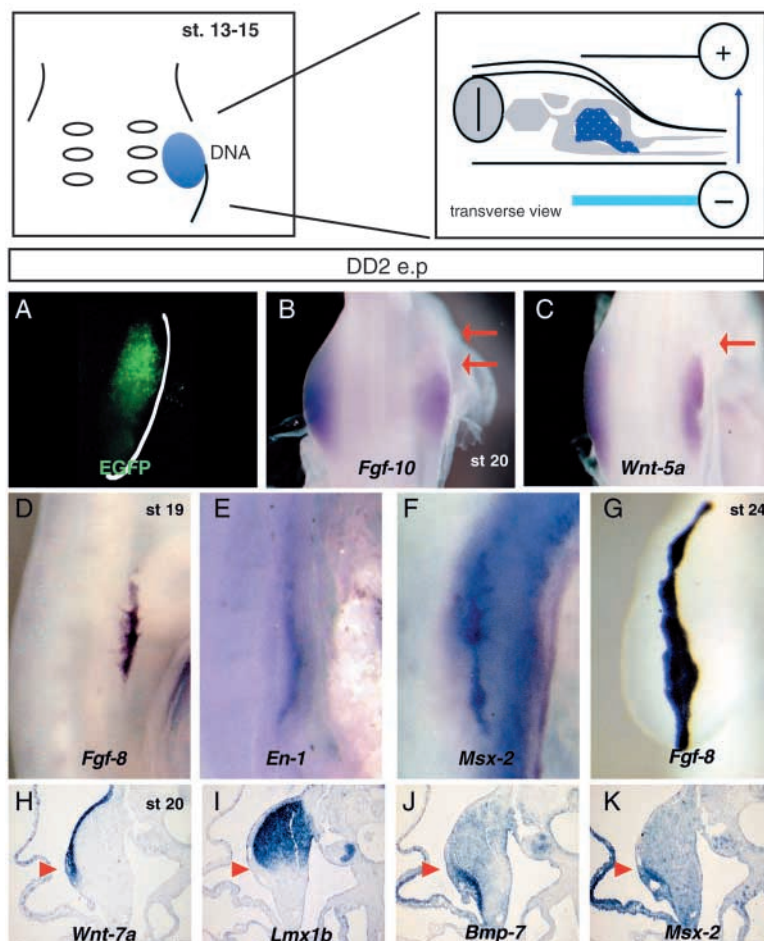


Fig. 3. Misexpression of DD2 in the limb mesenchyme by injecting plasmid solutions in the lateral plate mesoderm. Diagrams show the experimental design of electroporation. (A) We misexpressed the EGFP gene to monitor the expression of transgenes in the mesenchyme. (B) DD2 misexpression at stages 13-15 induced repression of *Fgf10* expression at stage 20 (red arrows). (C) *Wnt5a* was also repressed (red arrow), with deformity of the AER. (D-F) At stage 19, expression of *Fgf8*, *En-1* and *Msx2* became unclear and distorted. (G) At stage 24, a broad and irregular AER was formed as judged by the *Fgf8*-positive domain, in which a *Fgf8*-negative line was observed. (H-K) At stage 20, *Wnt7a* and *Lmx1b* were expressed dorsally, and *Bmp7* and *Msx2* ventrally, without disturbance of the DV axis formation. Nonetheless, thickening of the ectoderm was observed near the margin of the expression of these markers (red arrowheads). Approximately 35% of the DD2-misexpressed limb buds displayed this phenotype in the AER ($n=156$).

When these limbs were allowed to develop further, polydactylous digits developed (Fig. 4L,M) and were arranged in a double row, with digits a, b and c formed in a line, and digits a' and b' in another (Fig. 4M). When stained with Alcian Blue, this double row appearance was evident (Fig. 4N-P). As misexpression of DD2 induced the split AER (Fig. 3G) and/or the invagination of the ventral epithelium, we speculated that digits were formed in a double row arrangement in the split AER and/or the separate two limb protrusions (Fig. 4J,K).

Dach1 and the PD axis of limb buds

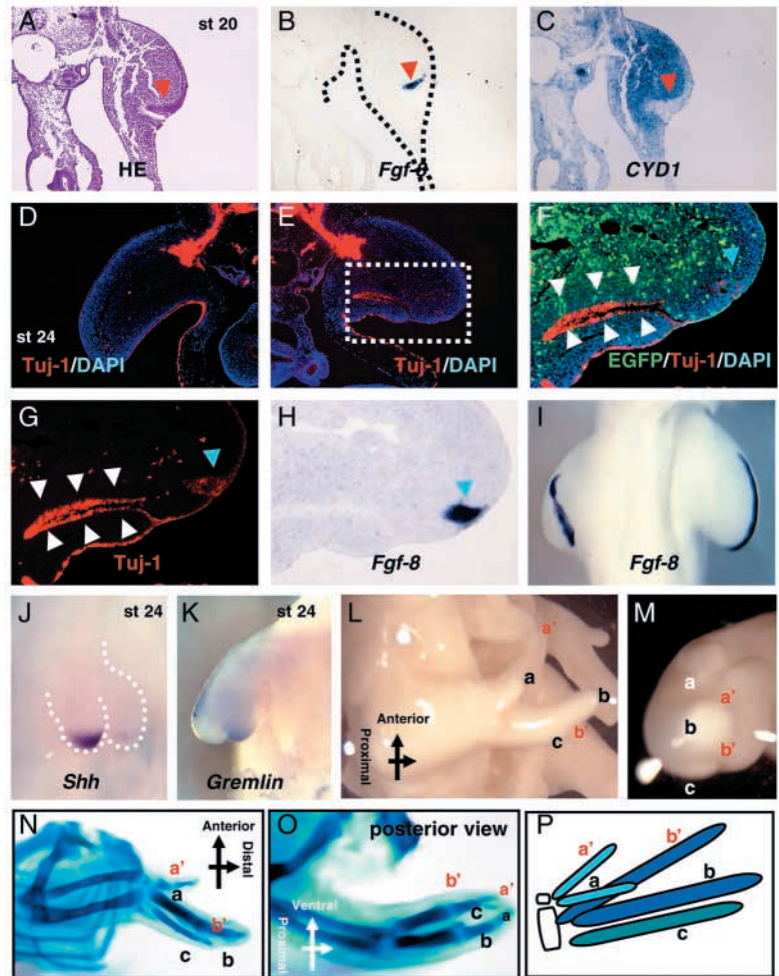
As reported previously, BMP signaling regulates pattern formation of limb buds along its PD axis (Capdevila et al., 1999). This suggests that Dach1 might be involved in this process, acting along with the BMP signaling pathway. To examine the effects of DD2 on the PD axis, we misexpressed DD2 in the entire limb mesoderm at stage 15 (Fig. 5A-F). In this case, expression of *Meis2* was induced in broader domains at stages 17 and 19 (Fig. 5B,E), compared with the normal expression on the control sides (Fig. 5C,F).

As reported previously, implantation of BMP4-soaked beads in the limb buds repressed *Meis2* expression, with a higher sensitivity in the proximal part and a lower sensitivity in the distal part (Fig. 5G,H). This indicates that phosphorylated Smad1 might make a repressor complex with Dach1 and other co-repressor factors, thereby inhibiting *Meis2* expression. When DD2 was misexpressed in the BMP4-implanted limb bud, this repression was cancelled (Fig. 5I). These data indicate that Dach1 is involved in the pattern formation of the limb buds along its PD axis, acting in the BMP signaling cascade.

We isolated a 700 bp putative regulatory region of the human *MEIS1* gene near its first exon. When this region was compared with the human *MEIS2* gene, it was highly conserved between these two genes, compatible with the similar expression patterns of these two *Meis* genes (Mercader et al., 2000). These results indicate that the *Meis1* and *Meis2* genes share similar regulatory elements crucial for their expression along the PD axis.

To investigate the roles of this region, we constructed a luciferase reporter by inserting the 5' 700 bp sequence of the human *MEIS1* gene upstream of the herpes simplex virus thymidine kinase (*TK*) promoter (Fig. 5J). This construct was transfected into HepG2 cells along with various combinations of effector plasmids (Fig. 5J). Addition of the BMP4 expression plasmid repressed this reporter weakly. Co-transfection of Dach1 and Sin3A super-repressed it, indicating that BMP signaling represses expression of *Meis1* acting with Smads, Dach1 and Sin3a. By contrast, co-expression of VP=Dach1 activated this reporter (Fig. 6J). These results suggest that Dach1 is involved in pattern formation along the PD axis, controlling the expression of *Meis* genes through the BMP signaling cascade.

Fig. 4. (A) At stage 20, invagination of the ectoderm was obtained (red arrowhead) in the DD2-misexpressed limb bud. (B) Expression of *Fgf8* was observed in the invaginated ectoderm (red arrowhead). (C) Cyclin D1 was expressed normally in the underlying mesenchyme. A red arrowhead indicates the invaginated epithelium. (D) In the normal limb bud, β III-tubulin proteins were detected by the TuJ1 antibody in both the ventral ectoderm and the motoneurons entering the limb. (E) In the DD2-misexpressed limb bud, β III-tubulin proteins were detected in the invaginated epithelium, suggesting that the invaginated ectoderm was derived from the ventral half. (F,G) The boxed shown in E was magnified. Clear TuJ1 staining was observed in the invaginated part (white arrowheads). In its distal-most end, thickening of the ectoderm was evident (blue arrowheads). EGFP proteins were visualized in green. (H) *Fgf8* was expressed in this thick ectoderm (blue arrowhead). (I) In a ventral view, expression of *Fgf8* was broad and flat. (J,K) At stage 24, two protrusions were formed with strong expression of *Shh* (J) and *Gremlin* (K) in the dorsal and the ventral protrusions, respectively. (L,M) When developed further, polydactylous limbs arose. Digits of such limbs were arranged in two rows, with digits a, b and c in one line, and digits a' and b' in another. A distal view was shown in M. (N,O) Skeletal patterns obtained by Alcian Blue staining. Lateral and posterior views are shown in N and O, respectively. (P) Schematic representation of the digit pattern in a dorsal view. Approximately 22% of the DD2-misexpressed limb buds displayed this phenotype ($n=27$).



Discussion

In this report, we highlight *Dach1* as an intracellular modulator of BMP signaling. In contrast to *Gremlin*, *Dach1* interacts with Smads to make a large repressor complex, thereby acting intracellularly. This suggests that BMP signaling is controlled both extra- and intracellularly. In previous studies, BMP signaling was manipulated only extracellularly, by *Gremlin*, *Noggin* and dominant-negative/constitutively active BMP receptors. By contrast, the intracellular signaling cascades of BMP signaling are multiple, involving Smad1/4-mediated transcriptional activation (Massague, 1998) and *ski/sno*-mediated repression (Wang et al., 2000). Recently, *Drosophila* Highwire, a putative RING finger E3 ubiquitin ligase, has been shown to bind to Smad protein to modulate BMP signaling (McCabe et al., 2004). Hence, nuclear events acting downstream of BMP signaling are multiple. Recently, *Dach1* has been shown to interact with Smad4 and NcoR. This suggests that *Dach1* modulates TGF β signaling (Wu et al., 2004), placing *Dach1* as a multiple modulator of Smad-mediated transcriptional control.

Recent studies have revealed that vertebrate *Dach* proteins interact with other transcription factors. In the limb bud, *Dach2* is expressed in migrating myoblast precursors (Heanue et al., 1999). *Dach2* interacts with *Eya2*, and *Eya2* interacts with *Six1*; therefore, a synergism among the *Dach2*, *Eya2* and *Six1* proteins regulates myogenic differentiation. In retinogenesis and pituitary development, *Dach1* and *Dach2* interact with *Six6*, HDAC, N-CoR and Sin3a to make a repressor complex, which then represses cyclin-dependent kinase inhibitors, such as *p27Kip1* (Li et al., 2002). In this report, *Dach1/2* were

shown to possess multiple interfaces; the DD1 domain interacts with *Six6*, HDAC and N-CoR, and the DD2 domain with Sin3a. In addition, the DD2 of *Dach2* interacts with *Eya2* (Heanue et al., 1999). In both cases, the *Dach* protein functions in the context of the DNA-binding protein *Six*, highlighting the *Dach* protein as a potent modulator of multiple transcriptional controls.

Dach1 was not expressed in the early stages of limb development (stages 13-17) (Heanue et al., 2002) (see Figs S1, S2 at <http://dev.biologists.org/supplemental>). *Dach1* expression began at stage 20 in the AER. This suggests that *Dach1* is not involved in the initiation of the AER or the DV axis determination; rather, it plays a role in its maintenance. Both in mouse and chick limbs, expression of *Dach1* was induced by implantation of beads soaked in several FGFs (Horner et al., 2002). This is compatible with our data showing that expression of *Fgf8* begins earlier than that of *Dach1* and supports the roles of *Dach1* in maintenance. When a constitutively active VP=*Dach1* was misexpressed in the pre-AER ectoderm, disruption of the AER and distal truncation were observed (Fig. 2); a similar change is induced by excess BMP signaling (Macias et al., 1997; Zou et al., 1997). When DD2 was misexpressed in the mesenchyme, repression of marker genes and deformation of the AER were also obtained (Fig. 3). This suggests that

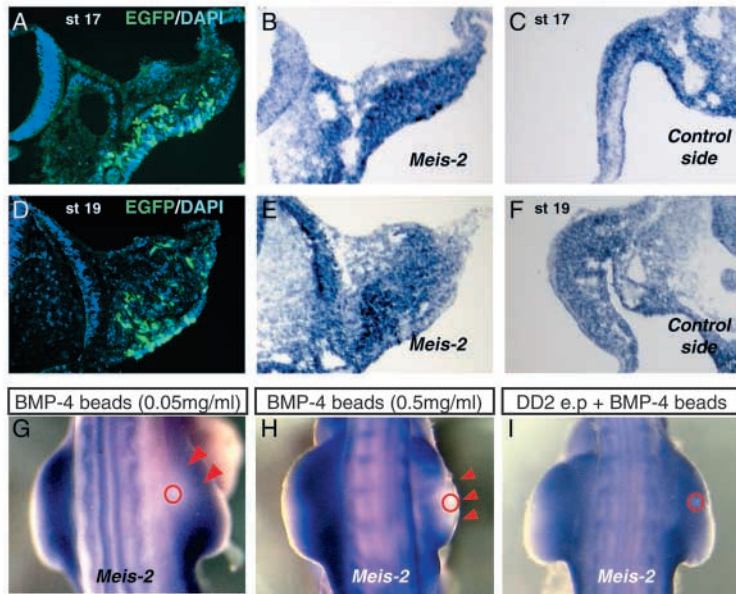
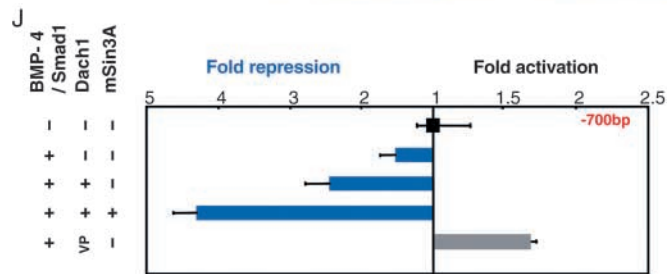


Fig. 5. (A-C) At stage 17, in the DD2-misexpressed limb, *Meis2* was induced (B) in an area where co-expressed EGFP proteins (shown in green) were detected (A). Normal expression was shown in C. (D-F) At stage 19, similar but more extensive induction of *Meis2* was observed. (G,H) Implantation of BMP4-soaked beads repressed *Meis2* expression (red arrowheads) in both a proximal area (G) and a distal end (H), with a deformity of the AER (H). (I) Misexpression of DD2 cancelled the BMP4-mediated repression of *Meis2*, with expansion of *Meis2* expression to the distal end. (J) A luciferase reporter plasmid containing 700 bp 5' region of human *MEIS1* was transfected into HepG2 cells, along with BMP4, Smad1, Dach1, VP=Dach1 and mouse Sin3a expression plasmids. Expression of BMP4, Smad1 and Dach1 repressed this reporter. This repression was enhanced by the addition of mouse Sin3a. By contrast, when VP=Dach1 was expressed, activation of this reporter was obtained.



Dach1 in the mesenchyme regulates the formation of the AER.

The actions of BMP molecules are antagonized by extracellular Gremlin. Nonetheless, BMP signaling is still weakly active in both the mesoderm and the ectoderm, as revealed by staining with an anti-phosphorylated Smad protein antibody (data not shown). This suggests that the attenuated BMP signals play a repressive role with Smads, Sin3a and Dach1. In contrast to Gremlin, Dach1 regulates the transcription of putative target genes, leaving other signaling cascades, such as p38 MAP kinase, intact (Kozawa et al., 2002). This might create different signaling contexts in the limb bud. When BMP signaling is shut off by forced expression of Gremlin, Noggin or dominant-negative BMP receptors, both the Smad/Dach1 pathway and the MAP kinase pathway are affected. By contrast, DD2 and VP=Dach1 affect only Smad-mediated transcription. In addition, Dach1 was reported to contain a DNA-binding motif (Kim et al., 2002), suggesting that complex formation of Dach1 and Smads might be influenced by sequences near the Smad-binding motif. Consequently, genes that contain only the Smad-binding motif might be activated by the Smad1/Smad4 complex. Hence, the transcriptional control of target genes might be dependent on the target sequences, although Smads play an essential role in both cases. The difference between extracellular and nuclear BMP antagonism might be related to the elongation of the ventral ectoderm, which was never observed with extracellular BMP antagonism. In addition, a balance between Dach1 and the phosphorylated Smad proteins might be important, as

excess BMP signaling induces nuclear accumulation of Smad proteins, which might change the stoichiometric ratio of phosphorylated Smad and Dach1 proteins, thereby affecting the transcriptional levels of the target genes.

Misexpression of VP=Dach1 induced expansion of *Meis2* expression in the distal domain, with intense expression in the anteroproximal area (see Figs S1, S2 at <http://dev.biologists.org/supplemental>). This suggests that Dach1 is involved in pattern formation along the PD axis of the limb bud. Consistent with this, implantation of BMP4-soaked beads repressed *Meis2* expression (Fig. 5G,H), suggesting that the Smads/Dach1 complex represses *Meis2*. When DD2 was misexpressed, repression of *Meis2* was cancelled (Fig. 5I), probably because DD2 abrogated the formation of the repressor complex. *Drosophila* data indicate that Dachshund is involved in pattern formation of the leg along its PD axis. Hence, the functional link between BMP/Dpp and Dach1/Dachshund is highly conserved in both invertebrates and vertebrates, placing Smad/Mad as a junction of signaling.

Recently, the mouse *Dach1* gene was successfully knocked out, showing no overt morphological changes (Davis et al., 2001). This suggests that there might be genetic redundancy, because expression of mouse *Dach2* overlaps with that of *Dach1* (Davis et al., 2001; Heanue et al., 1999). In addition, chick Ski, which also binds to Smad proteins to repress BMP-mediated transcription (Wang et al., 2000), is expressed in the developing limb buds (Dai et al., 2002). This suggests that multiple mechanisms of transcriptional control operate in the limb buds.

Our data have shown that Dach1 plays pivotal roles as an intracellular BMP antagonist and contributes to pattern formation along the PD axis and maintenance of the AER. In addition, our data have revealed that a direct interaction among Dach1, Smads and co-repressors is essential. Hence, our data uncover a novel set of interactions, introducing a new paradigm in the regulation of limb outgrowth. Further molecular dissection of Dach1 should provide novel insight into the

highly conserved genetic program operating in both invertebrate and vertebrate appendages.

We thank Drs S. Ishii, A. E. Munsterberg, C. Tabin, K. Miyazono, A. Kuroiwa, S. Noji, J. C. Izpisua-Belmonte and N. Ueno for probes and plasmids. This work was supported by a Grant-in-Aid for Scientific Research on Priority Areas (C) and Creative Basic Research from the Ministry of Education, Science, Sports and Culture of Japan (T.O.); and by the Toray Science Foundation (T.O.).

References

- Ahn, K., Mishina, Y., Hanks, M. C., Behringer, R. R. and Crenshaw, E. B., III. (2001). BMPR-IA signaling is required for the formation of the apical ectodermal ridge and dorsal-ventral patterning of the limb. *Development* **128**, 4449-4461.
- Barrow, R. J., Thomas, R. K., Boussadia-Zahui, O., Moore, R., Kemler, R., Caoecchi, R. M. and McMahon, P. A. (2003). Ectodermal *Wnt/β-catenin* signaling is required for the establishment and maintenance of the apical ectodermal ridge. *Genes Dev.* **17**, 394-409.
- Borsani, G., DeGrandi, A., Ballabio, A., Bulfone, A., Bernard, L., Banfi, S., Gattuso, C., Mariani, M., Dixon, M., Donnai, D. et al. (1999). EYA4, a novel vertebrate gene related to *Drosophila* eyes absent. *Hum. Mol. Genet.* **8**, 11-23.
- Capdevila, J. and Izpisua Belmonte, J. C. (2001). Patterning mechanisms controlling vertebrate limb development. *Annu. Rev. Cell Dev. Biol.* **17**, 87-132.
- Capdevila, J., Tsukui, T., Rodriguez Esteban, C., Zappavigna, V. and Izpisua Belmonte, J. C. (1999). Control of vertebrate limb outgrowth by the proximal factor *Meis2* and distal antagonism of BMPs by *Gremlin*. *Mol. Cell* **4**, 839-849.
- Chen, R., Amoui, M., Zhang, Z. and Mardon, G. (1997). Dachshund and eyes absent proteins form a complex and function synergistically to induce ectopic eye development in *Drosophila*. *Cell* **91**, 893-903.
- Cygan, J. A., Johnson, R. L. and McMahon, A. P. (1997). Novel regulatory interactions revealed by studies of murine limb pattern in *Wnt-7a* and *En-1* mutants. *Development* **124**, 5021-5032.
- Dai, P., Shinagawa, T., Nomura, T., Harada, J., Kaul, S. C., Wadhwa, R., Khan, M. M., Akimaru, H., Sasaki, H., Colmenares, C. et al. (2002). Ski is involved in transcriptional regulation by the repressor and full-length forms of Gli3. *Genes Dev.* **16**, 2843-2848.
- Davis, J. R., Shen, W., Sandler, I. Y., Heanue, A. T. and Mardon, G. (2001). Characterization of mouse *Dach2*, a homologue of *Drosophila dachshund*. *Mech. Dev.* **102**, 169-179.
- Davis, J. R., Shen, W., Sandler, I. Y., Amoui, M., Purcell, P., Maas, R., Ou, C., Vogel, H., Beaudet, L. A. and Mardon, G. (2001). *Dash1* mutant mice bear no gross abnormalities in eye, limb, and brain development and exhibit postnatal lethality. *Mol. Cell. Biol.* **21**, 1484-1490.
- Desplan, C. (1997). Eye development: governed by a dictator or a junta? *Cell* **91**, 861-864.
- Gonzalez-Crespo, S., Abu-Shaar, M., Torres, M., Martinez, A. C., Mann, R. S. and Morata, G. (1998). Antagonism between extradenticle function and Hedgehog signalling in the developing limb. *Nature* **394**, 196-200.
- Hammond, K. L., Hanson, I. M., Brown, A. G., Lettice, L. A. and Hill, R. E. (1998). Mammalian and *Drosophila dachshund* genes are related to the *Ski* proto-oncogene and are expressed in eye and limb. *Mech. Dev.* **74**, 121-131.
- Hata, A., Seoane, J., Lagna, G., Montalvo, E., Hemmati-Brivanlou, A. and Massague, J. (2000). OAZ uses distinct DNA- and protein-binding zinc fingers in separate BMP-Smad and Olf signaling pathways. *Cell* **100**, 229-240.
- Hayashi, H., Mochii, M., Kodama, R., Hamada, Y., Mizuno, N., Eguchi, G. and Tachi, C. (1996). Isolation of a novel chick homolog of *Serrate* and its coexpression with *C-Notch-1* in chick development. *Int. J. Dev. Biol.* **40**, 1089-1096.
- Heanue, T. A., Reshef, R., Davis, R. J., Mardon, G., Oliver, G., Tomarev, S., Lassar, A. B. and Tabin, C. J. (1999). Synergistic regulation of vertebrate muscle development by *Dach2*, *Eya2*, and *Six1*, homologs of genes required for *Drosophila* eye formation. *Genes Dev.* **13**, 3231-3243.
- Heanue, T. A., Davis, R. J., David, H. R., Kispert, A., McMahon, A. P., Mardon, G. and Tabin, C. J. (2002). *Dach1*, a vertebrate homologue of *Drosophila dachshund*, is expressed in the developing eye and ear of both chick and mouse and is regulated independently of *Pax* and *Eya* genes. *Mech. Dev.* **111**, 75-87.
- Horner, A., Shum, L., Ayres, J. A., Nonaka, K. and Nuckolls, G. H. (2002). Fibroblast growth factor signaling regulates *Dach1* expression during skeletal development. *Dev. Dyn.* **225**, 35-45.
- Johnson, R. L. and Tabin, C. J. (1997). Molecular models for vertebrate limb development. *Cell* **90**, 979-990.
- Kim, S., Zang, R., Braunstein, E. S., Joachimial, A., Gvekl, A. and Hogde, A. (2002). Structure of the retinal determination protein *Dachshund* reveals a DNA binding motif. *Structure* **10**, 787-795.
- Koshiba-Takeuchi, K., Takeuchi, J. K., Matsumoto, K., Momose, T., Uno, K., Hoepker, V., Ogura, K., Takahashi, N., Nakamura, H., Yasuda, K. et al. (2000). *Tbx5* and the retinotectum projection. *Science* **287**, 134-137.
- Kozawa, O., Hatakeyama, D. and Uematsu, T. (2002). Divergent regulation by p44/p42 MAP kinase and p38 MAP kinase of bone morphogenetic protein-4-stimulated osteocalcin synthesis in osteoblasts. *J. Cell. Biochem.* **84**, 583-589.
- Kozmik, Z., Pfeffer, P., Kralova, J., Paces, J., Paces, V., Kalousova, A. and Cvekl, A. (1999). Molecular cloning and expression of the human and mouse homologues of the *Drosophila dachshund* gene. *Dev. Genes Evol.* **209**, 537-545.
- Li, X., Perissi, V., Liu, F., Rose, D. W. and Rosenfeld, M. G. (2002). Tissue-specific regulation of retinal and pituitary precursor cell proliferation. *Science* **297**, 1180-1183.
- Lopez-Rios, J., Gallardo, M. E., Rodriguez de Cordoba, S. and Bovolenta, P. (1999). *Six9* (*Optx2*), a new member of the six gene family of transcription factors, is expressed at early stages of vertebrate ocular and pituitary development. *Mech. Dev.* **83**, 155-159.
- Macias, D., Ganan, Y., Sampath, T. K., Piedra, M. E., Ros, M. A. and Hurler, J. M. (1997). Role of BMP-2 and OP-1 (*BMP-7*) in programmed cell death and skeletogenesis during chick limb development. *Development* **124**, 1109-1117.
- Mardon, G., Solomon, N. M. and Rubin, G. M. (1994). *dachshund* encodes a nuclear protein required for normal eye and leg development in *Drosophila*. *Development* **120**, 3473-3486.
- Martin, G. R. (1998). The roles of FGFs in the early development of vertebrate limbs. *Genes Dev.* **12**, 1571-1586.
- Massague, J. (1998). TGF-beta signal transduction. *Annu. Rev. Biochem.* **67**, 753-791.
- McCabe, B. D., Hom, S., Aberle, H., Fetter, R. D., Marques, G., Haerry, T. E., Wan, H., O'Connor, M. B., Goodman, C. S. and Haghghi, A. P. (2004). *Highwire* regulates presynaptic BMP signaling essential for synaptic growth. *Neuron* **41**, 891-905.
- Mercader, N., Leonardo, E., Elisa, M., Martinez, A. C., Ros, M. A. and Torres, M. (2000). Opposing RA and FGF signals control proximodistal vertebrate limb. *Development* **127**, 3961-3970.
- Merino, R., Rodriguez-Leon, J., Macias, D., Ganan, Y., Economides, A. N. and Hurler, J. M. (1999). The BMP antagonist *Gremlin* regulates outgrowth, chondrogenesis and programmed cell death in the developing limb. *Development* **126**, 5515-5522.
- Mishima, N. and Tomarev, S. (1998). Chicken *Eyes absent 2* gene: isolation and expression pattern during development. *Int. J. Dev. Biol.* **42**, 1109-1115.
- Oliver, G., Mailhos, A., Wehr, R., Copeland, N. G., Jenkins, N. A. and Gruss, P. (1995). *Six3*, a murine homologue of the *sine oculis* gene, demarcates the most anterior border of the developing neural plate and is expressed during eye development. *Development* **121**, 4045-4055.
- Pignoni, F., Hu, B., Zavitz, K. H., Xiao, J., Garrity, P. A. and Zipursky, S. L. (1997). The eye-specification proteins *So* and *Eya* form a complex and regulate multiple steps in *Drosophila* eye development. *Cell* **91**, 881-891.
- Pizette, S. and Niswander, L. (1999). BMPs negatively regulate structure and function of the limb apical ectodermal ridge. *Development* **126**, 883-894.
- Pizette, S., Abate-Shen, C. and Niswander, L. (2001). BMP controls proximodistal outgrowth, via induction of the apical ectodermal ridge, and dorsoventral patterning in the vertebrate limb. *Development* **128**, 4463-4474.
- Quiring, R., Walldorf, U., Kloter, U. and Gehring, W. J. (1994). Homology of the *eyeless* gene of *Drosophila* to the *Small eye* gene in mice and *Aniridia* in humans. *Science* **265**, 785-789.
- Rubin, L. and Saunders, J. W., Jr (1972). Ectodermal-mesodermal interactions in the growth of limb buds in the chick embryo: constancy and temporal limits of the ectodermal induction. *Dev. Biol.* **28**, 94-112.
- Schwabe, J. W., Rodriguez-Esteban, C. and Izpisua Belmonte, J. C. (1998). Limbs are moving: where are they going? *Trends Genet.* **14**, 229-235.
- Takeuchi, J. K., Koshiba-Takeuchi, K., Suzuki, T., Kamimura, M., Ogura, K. and Ogura, T. (2003). *Tbx5* and *Tbx4* trigger limb initiation through activation of the *Wnt/Fgf* signaling cascade. *Development* **130**, 2729-2739.

- Wang, W., Mariani, F. V., Harland, R. M. and Luo, K.** (2000). Ski represses bone morphogenic protein signaling in *Xenopus* and mammalian cells. *Proc. Natl. Acad. Sci. USA* **97**, 14394-14399.
- Wawersik, S. and Maas, R. L.** (2000). Vertebrate eye development as modeled in *Drosophila*. *Hum. Mol. Genet.* **9**, 917-925.
- Wilkinson, D. G. and Nieto, M. A.** (1993). Detection of messenger RNA by in situ hybridization to tissue sections and whole mounts. *Methods Enzymol.* **225**, 361-373.
- Wu, K., Yang, Y., Wang, C., Davoli, M. A., D'Amico, M., Li, A., Cveklova, K., Kozmik, Z., Lisanti, M. P., Russell, R. G. et al.** (2004). DACH1 inhibits TGF-beta signaling through binding Smad4. *J. Biol. Chem.* **278**, 51673-51684.
- Yokouchi, Y., Sakiyama, J., Kameda, T., Iba, H., Suzuki, A., Ueno, N. and Kuroiwa, A.** (1996). BMP-2/-4 mediate programmed cell death in chicken limb buds. *Development* **122**, 3725-3734.
- Zou, H., Wiese, R., Massague, J. and Niswander, L.** (1997). Distinct role of type I bone morphogenetic protein receptors in the formation and differentiation of cartilage. *Genes Dev.* **11**, 2129-2203.
- Zuniga, A., Haramis, A. P., McMahon, A. P. and Zeller, R.** (1999). Signal relay by BMP antagonism controls the SHH/FGF4 feedback loop in vertebrate limb buds. *Nature* **401**, 598-602.
- Zwilling, E.** (1956). Interaction between limb bud ectoderm and mesoderm in the chick embryo. IV. Experiments with a wingless mutant. *J. Exp. Zool.* **132**, 241-253.